ingegneria sismica
International Journal of Earthquake Engineering
Anno XLIII - Num. 1 - 2026

Testing Method for Evaluating the Sensitivity and Reliability of Directional Protection Devices for High-Penetration Distributed Power Supply Distribution Networks

Xuepeng Mou[1,*], *Jian Wang*[1] *and Qingsheng Li*[1]

[1] Guizhou Power Grid Co., Ltd. Power Grid Planning and Research Center, Guiyang, Guizhou, 550003, China

SUMMARY: *In order to make a scientific analysis and increase the adaptability of the protective device, this paper introduces an assessment method based on loop analysis and Monte Carlo simulation. First, loop analysis is used to detect any variation in operating parameters in the distribution network. A voltage sensitivity matrix is established in order to get the sensitivity network loss for the distributed generation connected to the grid. A better three-point estimation algorithm is introduced for simplification of the probability calculations while a third-order polynomial normal transformation is used to standardize the arbitrary random variables. Moreover, the reliability evaluation of the protection device in the distribution network is conducted using the sequential Monte Carlo approach. At last, the probability distribution function of random variables is determined using the Edgeworth series expansion method. With the help of sensitivity assessment method based on loop analysis, dynamic detection of weak areas of the protective device can be carried out in the distribution network. Relative to the traditional Monte Carlo simulation, the reliability assessment of distribution network protection under the Monte Carlo simulation has a relatively small deviation and reaches up to 0.000% in the ASAI index.*

KEYWORDS: *loop analysis method; Monte Carlo method; improved three-point estimation method; Edgeworth series; distributed power sources*

1 Introduction

Distributed generation (DG) is a new way of power generation that is encouraged by world policies on environmental sustainability and technology innovation [1, 2]. At the end of the twentieth century, electric power companies were operating under the principle of centralized power generation. This means that power was generated in large central stations and delivered to consumers using a high voltage grid and a hierarchically structured network of high, medium, and low voltage distribution grids. Power was flowing in one direction from the generating stations to the grid and then to the consumers [3-6]. With the inclusion of distributed energy sources into the distribution grid, there have been considerable changes in this pattern of power generation. Power generation is becoming more localized and closer to consumers. However, the integration of distributed power generation with the distribution grid has added complexities in its management [7-10].

The inclusion of DG into the electrical grid system gives rise to several impacts on the distribution system. The impacts are dependent on the states of the distribution system as well

*mxp_gzdw@163.com
https://doi.org/10.65102/is2026490
Published: 30 April, 2026

as DG. Conventional distribution systems have a radial structure with a single source of electricity and hence require particular relay protection settings [11-14]. The inclusion of DG results in a change in the topology of the distribution system. In case of faults in the distribution system, the system will provide fault currents to the fault point. The DG sources will inject fault currents into the fault point as well. Therefore, the injection causes a change in the fault current levels at the nodes of the distribution system, affecting the protection relay operation [15-18]. Also, the nature, installation sites, and capacities of DG can impact the relay protection in the distribution system [19, 20]. For safety and reliability of distribution lines, directional protection devices should be installed alongside other electrical devices. Typical protection devices used in low-voltage distribution lines include fuses and circuit breakers. Since sensitivity and reliability are critical aspects in choosing protection devices, these two attributes should be evaluated and tested [21-24].

The integration of distributed power sources may significantly alter the sensitivity of protection devices and the reliability of the system. To enhance the adaptability of protection devices in complex distribution network environments, this paper introduces an evaluation method based on voltage fluctuation theory and loop analysis to precisely identify and protect the weak links in distribution network protection devices. In terms of reliability assessment, this paper proposes an improved sequential Monte Carlo probability assessment method, which incorporates improved three-point estimation methods and Edgeworth series methods, and embeds a dynamic island division mechanism. The applicability of this method is studied on the improved IEEE-RBTS Bus6 F4 feeder system.

2 Distribution network sensitivity analysis method based on loop analysis

2.1 Voltage Fluctuation Theory

Due to changes in the power flow distribution in the distribution network, this indirectly causes fluctuations in the node voltages on the distribution network. If we consider two nodes in the system as a and b respectively, with the current flowing from a to b, Ua and Ub represent the voltages at the two nodes. $R+jX$ represents the impedance between the two nodes, while Pb and Qb denote the active power and reactive power at node b, respectively. As shown in Figure 1.

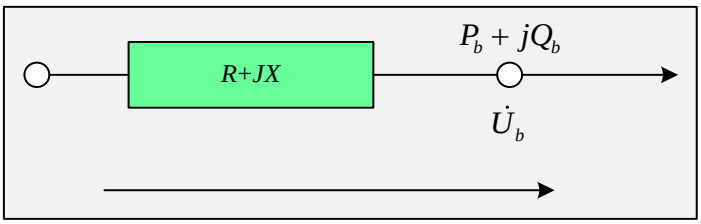

Figure 1: Contour circuit

You can then obtain the voltage loss formula (1):

$$\Delta U = \Delta U_z + \Delta U_h = \left(\frac{P_b - JX_b}{U_b} \right) (R + JX) \tag{1}$$

In this formula, Δ_U and Δ_{Uh} represent the vertical and horizontal components of voltage changes, respectively. By ignoring the horizontal components of voltage at the two nodes, we obtain formula (2).

$$\Delta U = \Delta U_z = \frac{P_b R + Q_b X}{U_b} \tag{2}$$

2.2 Method for analyzing the effects before and after connecting distributed power sources

To begin with, two simpler distribution network layouts are considered. In the first layout, there is a distributed power source present, and in the second, there is no presence of such a distributed power source. Next, the plane effects resulting from the access of the distributed power source are studied. The circuit diagram of the distributed power source is represented in Figure 2, and the circuit diagram of the absence of distributed power source is represented in Figure 3.

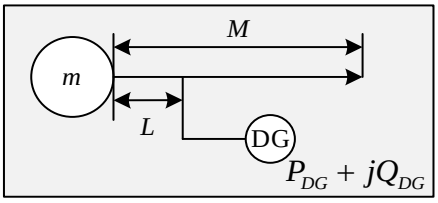

Figure 2: Connects to distributed power rendering

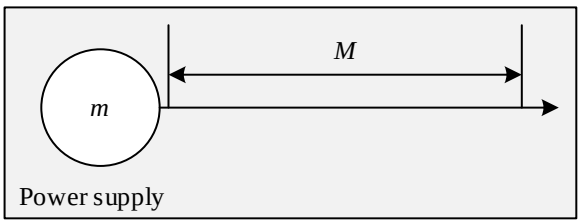

Figure 3: Does not access distributed power rendering

Since the impact of distributed power sources on voltage is relatively small after their integration, the effect on voltage can be neglected. In loop analysis, the voltages are equal. The capacity of the distributed power source is set to $P_{\mathrm{DG}} + \mathrm{j}Q_{\mathrm{DG}}$, and the line impedance in loop analysis is set to $R + \mathrm{j}X$. The length between the distributed power source and the power source is L between the distributed power source and the power source, and the length between the power source and the load end is M, it can be determined that the line losses in the distribution network are primarily composed of the line losses between the node and the distributed power source, as well as the line losses from the distributed power source to the load end, which are set as P_1 and P_2, respectively, thereby deriving equations (3), (4), and (5).

$$P = \frac{P_{load}^2 + Q_{load}^2}{U^2}\left(R + JX\right)M \tag{3}$$

$$P_1 = \frac{(P_{load} - P_{DG})^2 + (Q_{load} + Q_{DG})^2}{U^2}(R + JX)L \tag{4}$$

$$P_2 = \frac{(P_{load}^2 + Q_{load}^2)^2}{U^2}(R + JX)(M - L) \tag{5}$$

In view of the above formula, it implies that after the incorporation of the distributed power sources within the distribution system, the line losses tend to be highly dependent on the location, size, and generation capability of the said distributed power sources. Where the load size happens to be twice the size of the distributed power source and where the distributed power source size is smaller than the load size, there will be some reduction in line losses in the distribution network. However, if the size of the distributed power source exceeds the load size, then the line losses will be increased.

2.3 Circuit Analysis Methods

Based on loop analysis [25], the branch association matrix is incorporated. The concept of matrix B is as follows: when Bij equals 1, the branch is in the loop and the direction is the same; when Bij equals -1, the branch is in the loop but the direction is opposite; when Bij equals 0, the branch is not in the loop.

There are two principles for numbering distribution networks: ① Set the nodes in the distribution network to 0, with node 0 as the starting point of the distribution network, and another node i as the focal point, then mark i; ② Determine the starting and ending points of the branch nodes based on the direction of the branches, and number them according to the standard branches. As shown in Figure 4.

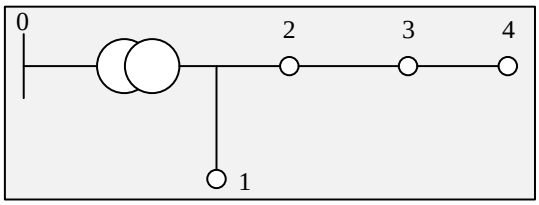

Figure 4: Node distribution grid diagram

Based on this figure, we can obtain the back-linkage correlation matrix B:

$$\{B\} = \begin{matrix} Z_1 & 0 & 0 & 0 \\ Z_1 & Z_2 & 0 & 0 \\ Z_1 & Z_2 & Z_3 & 0 \\ Z_1 & 0 & 0 & Z_4 \end{matrix} \tag{6}$$

After introducing the return impedance matrix Z_{LN}, the following results are obtained:

$$\{Z_{LK}\} = \begin{matrix} Z_1 & 0 & 0 & 0 \\ Z_1 & Z_2 & 0 & 0 \\ Z_1 & Z_2 & Z_3 & 0 \\ Z_1 & 0 & 0 & Z_4 \end{matrix} \tag{7}$$

After splitting, we obtain $\{Z_{LN}\} = \{R_{LN}\} + J\{X_{LN}\}$ (R_{LN} denotes the loop resistance

matrix, and X_{LN} denotes the loop reactance matrix).

When the voltage at node 0 and the voltages of the nodes in the distribution network remain constant, the corresponding equation formula without distributed power sources is derived. Equation (8) demonstrates it.

$$\begin{pmatrix} U_0 - U_1 = Z_1 I_1 \\ U_0 - U_2 = I_1 Z_1 + I_2 Z_2 \\ U_0 - U_3 = I_1 Z_1 + I_2 Z_2 + I_3 Z_3 \\ U_0 - U_4 = I_1 Z_1 + I_4 Z_4 \end{pmatrix} \tag{8}$$

The equation formula for connecting distributed power sources is shown in Formula (9).

$$\begin{pmatrix} U_0 - U_1' = Z_1 I_1' \\ U_0' - U_2' = I_1' Z_1 + I_2' Z_2 \\ U_0 - U_3' = I_1' Z_1 + I_2' Z_2 + I_3' Z_3 \\ U_0 - U_4' = I_1' Z_1 + I_4' Z_4 \end{pmatrix} \tag{9}$$

Combining the two formulas yields formula (10).

$$\begin{pmatrix} \Delta U_1 \\ \Delta U_2 \\ \Delta U_3 \\ \Delta U_4 \end{pmatrix} = - \begin{pmatrix} Z_1 & 0 & 0 & 0 \\ Z_1 & Z_2 & 0 & 0 \\ Z_1 & Z_2 & Z_3 & 0 \\ Z_1 & 0 & 0 & Z_4 \end{pmatrix} \begin{pmatrix} \Delta I_1 \\ \Delta I_2 \\ \Delta I_3 \\ \Delta I_4 \end{pmatrix} \tag{10}$$

In this formula, ΔU_i represents the voltage change matrix at the loop analysis node, and ΔI_i represents the branch current change matrix in the loop analysis.

Analysis of both approaches reveals that once the distributed energy sources are integrated into the distribution network, there is no change in the topology of the network or the impedance of the lines. Differences at the nodes are caused by differences in the current in the branches. The addition of distributed energy sources leads to changes in the currents of the branches, changing the initial single-source distribution network into a multi-source one. However, distributed energy sources contribute to the network's flow. However, distributed power sources also feed back the actual current conditions to all nodes in the network. Under such circumstances, the nodes where distributed power sources are connected are treated as the end nodes of the line segments, thereby exerting a certain influence on the current in the loop, becoming the key factor in the changes of distribution network parameters. The current sensitivity matrix node voltage in the loop is represented as $U_i = U_i \angle 0$, so $\{\Delta I_i\} = \{\Delta I_{zi}\} - j\{\Delta I_{hi}\}$ is used to construct the sensitivity matrices for the longitudinal and transverse components of the current, as shown in Equations (11) and (12).

$$\{\Delta I_{zi}\} = \{U_i / I\} \# \{B^T\} \{\Delta P_{zi}\} \tag{11}$$

$$\{\Delta I_{hi}\} = \{U_i / I\} \# \{B^T\} \{\Delta Q_{zi}\} \tag{12}$$

In these two formulas, $\{U_i / I\}$ represents the one-dimensional column vector of the voltage at the node, ΔP_{zi} represents the one-dimensional column vector of the power change at the node after connecting the distributed power source, ΔQ_{zi} represents the one-dimensional column vector of the reactive power change after connecting the distributed power source, and # denotes matrix multiplication.

2.4 Sensitive construction method for voltage network loss

First, we analyze the sensitivity matrix formula for the longitudinal component of voltage in the node, as shown in Formula (13).

$$\{\Delta U_{zi}\} = -\{R_{LN}\}\{\Delta I_{zi}\} - \{X_{LN}\}\{\Delta I_{hi}\} \tag{13}$$

In this formula, RLN represents the resistance matrix in the loop current, and XLN represents the reactance matrix in the loop current. The construction process is roughly divided into the following four steps. ① First, the initial data in the line must be clearly defined; ② Next, the topology structure of the distribution network is used to construct the correlation matrix of the loop DC, the resistance matrix in the loop DC, and the reactance matrix in the loop DC; ③ Subsequently, the sensitivity matrix of the longitudinal and transverse components of the current is constructed; ④ Finally, the longitudinal component matrix of the node voltage is constructed.

Next, the sensitivity matrix of the line loss is analyzed to obtain formula (14).

$$\begin{aligned}\{\Delta P_{Li}\} = \{&(\Delta P_i / U_i)\#(2P_i / U_i) + (\Delta P_i / U_i) \\ &+ (\Delta Q^i / U_i)\#(\Delta 2Q_i / U_i + \Delta Q_i / U_i)\}\#\{R_i\}\end{aligned} \tag{14}$$

In this formula, the power change parameters in the branch can be obtained, where # denotes matrix multiplication. The construction process consists of the following five steps: ① First, identify the one-dimensional column vector representing power at the branch node, and multiply it by the associated matrix of the loop DC current to obtain the initial node power matrix; ② Calculate the initial current horizontal component matrix and current vertical component matrix by using the initial node branch injection nodes and the corresponding node voltage matrix; ③ Understand the impedance in the line and construct a one-dimensional column vector; ④ Understand the line loss sensitivity matrix [26]; ⑤ Understand the network loss sensitivity.

3 Probabilistic reliability assessment of distribution networks based on the Monte Carlo method

3.1 Theoretical basis for probabilistic reliability assessment of distribution networks

3.1.1 Improving the three-point estimation method

The three-point estimation method [27] is a sampling technique where the feature points are chosen based on the probability and statistic characteristics of random variables. By doing such, it avoids the need to model and mathematically transform the process which makes it simple

and easier to execute. The use of even a small number of deterministic computations can result in comparatively high computational accuracy. To enhance the computational accuracy of the three-point estimation method, this paper applies the concept of probability theory, namely, the 3σ rule along with the concepts of normal distribution theory. Each input variable X_i has some edge points that are taken into account due to the properties of the edge sample data.

First, for the n-dimensional input variable $X'=\left(X_1,X_2,\cdots,X_n\right)$, the mathematical expectation μ_i, standard deviation σ_i, skewness coefficient $\lambda_{i,3}$, and kurtosis coefficient $\lambda_{i,4}$ of $X_i\left(i=1,2,\cdots,n\right)$ are calculated. The estimated points for X_i are chosen as $X_{i,k}=\mu_i+\xi_{i,k}\sigma_i\left(k=1,2,\cdots,5\right)$, When $k=1,2,3$, $X_{i,k}$ is the estimated point selected by the traditional three-point estimation method; when $k=4,5$, $X_{i,k}$ is the newly added estimated point by the improved three-point estimation method. The position coefficients and weight coefficients are one-to-one with the estimated points.

The position coefficient of X_i is:

$$\begin{cases}\xi_{i,1}=\lambda_{i,3}/2+\sqrt{\lambda_{i,4}-3\lambda_{i,3}^2/4}\\ \xi_{i,2}=0\\ \xi_{i,3}=\lambda_{i,3}/2-\sqrt{\lambda_{i,4}-3\lambda_{i,3}^2/4}\\ \xi_{i,4}=\sqrt{n}\\ \xi_{i,5}=-\sqrt{n}\end{cases} \tag{15}$$

The weight coefficient of $X_{i,k}$ measures the importance of each estimated point in the output variable, that is:

$$\begin{cases}p_{i,1}=\dfrac{1}{\xi_{k,1}(\xi_{k,1}-\xi_{k,3})}\\ p_{i,2}=\dfrac{2n-1}{2n}-\dfrac{1}{\lambda_{i,4}-\lambda_{i,3}^2}\\ p_{i,3}=\dfrac{-1}{\xi_{k,1}(\xi_{k,1}-\xi_{k,3})}\\ p_{i,4}=p_{i,5}=\dfrac{1}{4n}\end{cases} \tag{16}$$

Then, take out the estimated points $X_{i,k}$ of X_i one by one, combine them with the expected values of the remaining variables $X_j\left(j\neq i\right)$, and form an estimated point sample. The final sample generated is:

$$X=\begin{bmatrix} X_{1,1} & X_{1,3} & X_{1,4} & X_{1,5} & \cdots & \mu_1 \\ \mu_2 & \mu_2 & \mu_2 & \mu_2 & \cdots & \mu_2 \\ \vdots & \vdots & \vdots & \vdots & \ddots & \vdots \\ \mu_n & \mu_n & \mu_n & \mu_n & \cdots & \mu_n \end{bmatrix}^T_{n\times(4n+1)} \tag{17}$$

Let the function $H(\cdot)$ represent the relationship between the input and output variables. Substitute the sample X into this function and perform multidimensional operations $Y=H(X)$ to obtain the m-dimensional output variable $Y=(Y_1,Y_2,\cdots,Y_m)$. Finally, combine the weight coefficients to calculate the vth-order origin matrix of the output variable Y:

$$\begin{aligned}\alpha_v=E(Y^v)=\sum_{i=1}^{n}\sum_{k=1}^{1,3,4,5}p_{i,k}\left[H(\mu_1,\cdots,X_{i,k},\cdots,\mu_n)\right]^v \\ +\sum_{i=1}^{n}p_{i,2}\left[H(\mu_1,\cdots,\mu_i,\cdots,\mu_n)\right]^v\end{aligned} \tag{18}$$

3.1.2 Third-order polynomial normal transformation

Three-point estimation technique utilizes digital feature sampling and hence produces a sample X where all variables are not correlated. Therefore, for this study, third order polynomial normal transformation will be applied in order to reintroduce the correlation between sample variables.

The third order polynomial normal transformation entails expressing the variables from any distribution in form of a polynomial expression using standard normal variable(s). The process does not involve any estimation of the probability distribution of the random variable. Third order polynomial normal transformation is easy to apply to discrete sample data. The basic idea behind third order polynomial normal transformation is that a non independent and non-normal random variable S_i can be approximated by using standard normal random variable Z_i such that:

$$S_i=a_{i,0}+a_{i,1}Z_i+a_{i,2}Z_i^2+a_{i,3}Z_i^3 \tag{19}$$

In the equation, $a_{i,0}$, $a_{i,1}$, $a_{i,2}$, and $a_{i,3}$ are the transformation coefficients of S_i, satisfying the conditions $a_{i,3}>0$ and $a_{i,2}^2-3a_{i,2}a_{i,3}\le 0$.

By performing a Cornish-Fisher series expansion, the formula for calculating the conversion coefficients using the numerical characteristics of S_i is obtained as follows:

$$\begin{cases} a_{i,0}=\mu_i-\sigma_i\lambda_{i,3}/6 \\ a_{i,1}=\sigma_i(33-3\lambda_{i,4})/24 \\ a_{i,2}=\sigma_i\lambda_{i,3}/6 \\ a_{i,3}=\sigma_i(\lambda_{i,4}-3)/24 \end{cases} \tag{20}$$

In the equation, μ_i, σ_i, $\lambda_{i,3}$, and $\lambda_{i,4}$ represent the expected value, standard deviation, skewness coefficient, and kurtosis coefficient of S_i, respectively.

Extend the above transformation to multiple dimensions. $S=(S_1,S_2,\cdots,S_n)$ is an n-dimensional set of independent and identically distributed random variables. The correlation coefficients between the elements of S can be described by the matrix ρ, where the elements $\rho_{ij}\left(i,j=1,2,\cdots,n\right)$ of ρ are the correlation coefficients between X_i and X_j. The independent standard normal random variables $Z=(Z_1,Z_2,\cdots,Z_n)$ correspond one-to-one with the elements of S. Let ρ_0 be the correlation coefficient matrix of Z, and ρ_{0ij} be the correlation coefficient between Z_i and Z_j. ρ_{ij} and ρ_{0ij} satisfy the following relationship:

$$\begin{aligned}6a_{i,3}a_{j,3}\rho_{0ij}^3+2a_{i,2}a_{j,2}\rho_{0ij}^2+(a_{i,1}+3a_{i,3})(a_{j,1}+3a_{j,3})\rho_{0ij}\\+(a_{i,0}+a_{i,2})(a_{j,0}+a_{j,2})-\rho_{ij}\sigma_i\sigma_j-\mu_i\mu_j=0\end{aligned}\tag{21}$$

Select solutions that satisfy $|\rho_{0ij}|\leq 1$ and $\rho_{ij}\rho_{0ij}\geq 0$ as values for ρ_{0ij}. Solve for all ρ_{0ij} to form ρ_0. ρ_0 is a symmetric matrix. Perform Cholesky decomposition on it to obtain the lower triangular matrix L_0, i.e.:

$$\rho_0=L_0L_0^T\tag{22}$$

In an independent standard normal space, use orthogonal transformation to convert X into non-independent standard normal random variables:

$$Z=L_0X\tag{23}$$

Calculate the non-independent, non-normal random variable S, where S represents the final system state sample that accounts for correlations and is representative of the system. Each column S_i of S denotes a specific element in the system, such as wind turbines, photovoltaic output, and load quantities at various load points. Each row of S represents a representative system state row generated.

To conclude, the numeric attributes of random variables represent key components of the third-degree polynomial normal transformation. For continuous variables with predetermined probability distributions and discrete variables with solely historical information, this transformation works well in handling variable correlations.

3.1.3 Edgeworth series expansion

The Edgeworth series [28] can approximate the probability distribution of any random variable using the standard normal distribution function. Compared to other asymptotic expansion series, the calculation process of this series is relatively simple and efficient.

By improving the three-point estimation method and the third-order polynomial normal transformation, the system state samples S are input into the system reliability calculation process $H\left(\cdot\right)$, yielding the output variables $Y=\left(Y_1,Y_2,\cdots,Y_m\right)$, where each dimension Y_i of Y represents the value of a single reliability metric at each sample point.

For convenience of explanation, let the value Y_i of a single reliability indicator at each estimated point sample be a random variable y. Before performing the Edgeworth series expansion, calculate the expected value μ_y and standard deviation σ_y of y, and standardize them to obtain the standardized variables:

$$\bar{y} = \frac{y - \mu_y}{\sigma_y} \tag{24}$$

The ith-order Hermite orthogonal polynomial $H_i(y)$ and the semi-invariant κ_i of y are important components of the Edgeworth series, respectively:

$$\begin{cases} H_0(y) = 1 \\ H_1(y) = y \\ H_{i+1}(y) = iH_i(y) - iH_{i-1}(y) \end{cases} \tag{25}$$

$$\kappa_v = \alpha_v - \sum_{j=1}^{v-1} C_{v-1}^{j-1} \kappa_j \alpha_{v-j} \tag{26}$$

In the formula, α_v is the vth moment of the random variable $\bar{y}$ at the origin.

According to the Edgeworth series expansion, the probability distribution function of the random variable y is:

$$F(y) = \int_y^{+\infty} \varphi(y)dy + \varphi(y)\sum_{i=3}^{+\infty} C_i H_{i-1}(y) \tag{27}$$

In the equation, $\varphi(\cdot)$ is the probability density function of the standard normal distribution; C_i is the coefficient of each term in the Edgeworth series.

The probability density function of y is obtained by differentiation:

$$f(y) = F'(y) = \varphi(\bar{y}) + \frac{\kappa_3}{3!}\varphi(\bar{y})H_3(\bar{y}) + \frac{\kappa_4}{4!}\varphi(\bar{y})H_4(\bar{y}) + \cdots \tag{28}$$

3.2 Probabilistic reliability calculation methods for distribution networks

Representative states of each sample are selected in this research through the refinement of the estimation of three points along with the use of a third order polynomial normal transformation. The next step involves using Monte Carlo simulations to obtain the index value for each sample and expanding the series to find out the probability distributions of each index.

3.2.1 Sequential Monte Carlo method for considering dynamic islanding in distribution networks

This paper selects four load point reliability indicators: failure rate λ (times/year), average power outage duration per failure r (hours/failure), annual average power outage time $U(h/a)$, and expected load point power shortage (ENS) $(kW \cdot h/a)$; Five system reliability metrics that are not correlated: average outage frequency (SAIFI) (times/(user·year)), system average outage duration metric (SAIDI) (hours/(user·year)), customer average outage duration metric (CAIDI) (hours/(outage-affected users·year)), average supply availability rate (ASAI) (%), , and System Energy Shortfall Expectation (ENS) $(kW \cdot h/a)$.

This paper calculates the Time to Failure (TTF) and Time to Repair (TTR) for each device based on the component failure model:

$$\begin{cases} t_{TTF} = -\ln(U_1 / \lambda) \\ t_{TTR} = -\ln(U_2 / \mu) \end{cases} \tag{29}$$

In the formula, λ and μ are the failure rate and repair rate of the equipment, respectively; U_1 and U_2 are random numbers uniformly distributed in the interval $[0,1]$.

The dynamic islanding mode of islanding division of the distribution system by using the sequential Monte Carlo scheme is utilized to identify the failed elements at every stage of sampling and reliability computation of the distribution system in Figure 5.

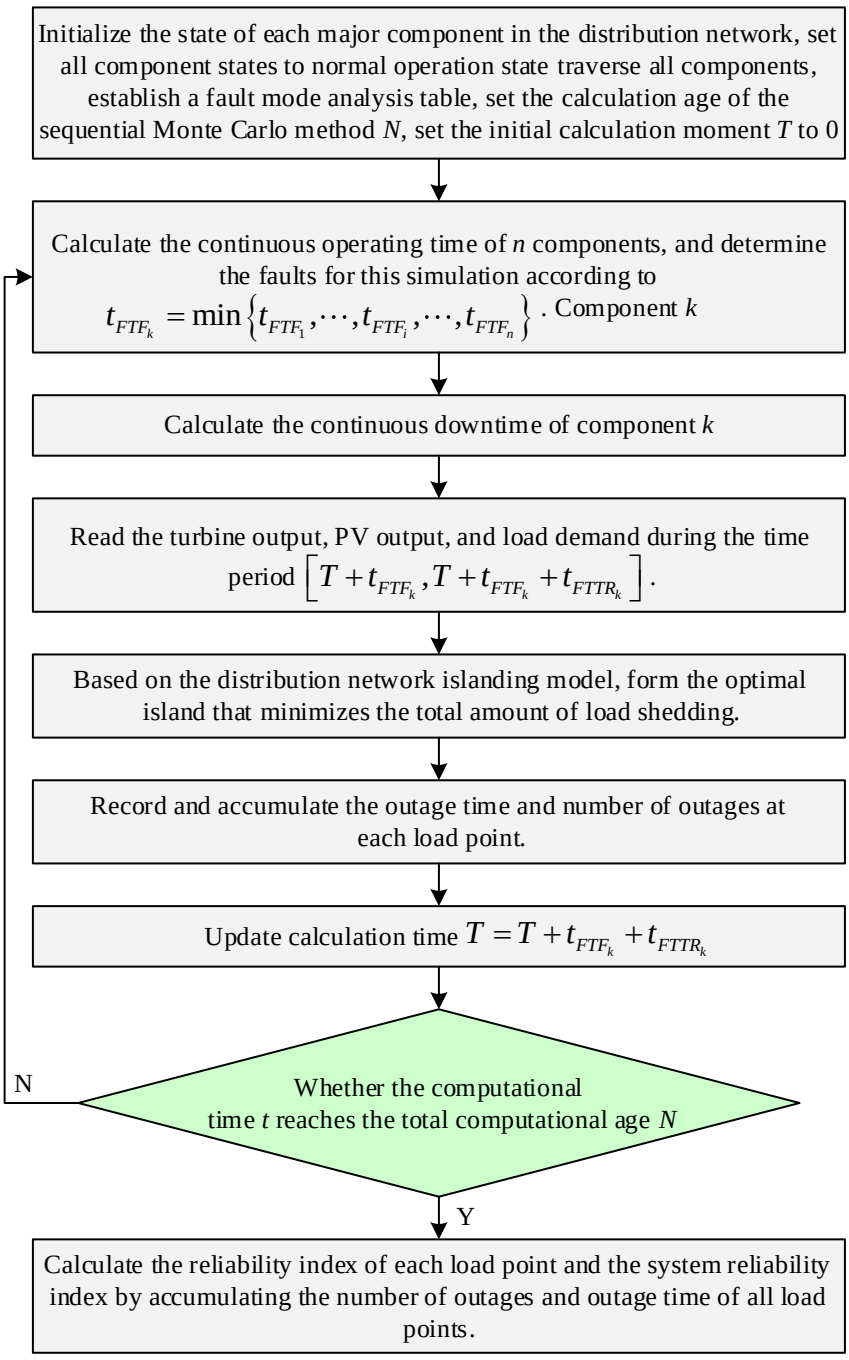

Figure 5: Distribution network considering dynamic islanding

3.2.2 Steps for calculating the probabilistic reliability of distribution networks

In light of the practical demands for evaluating reliability in the distribution network system, Figure 6 illustrates the probabilistic reliability analysis technique utilizing the three-point estimate approach along with the Edgeworth series expansion method.

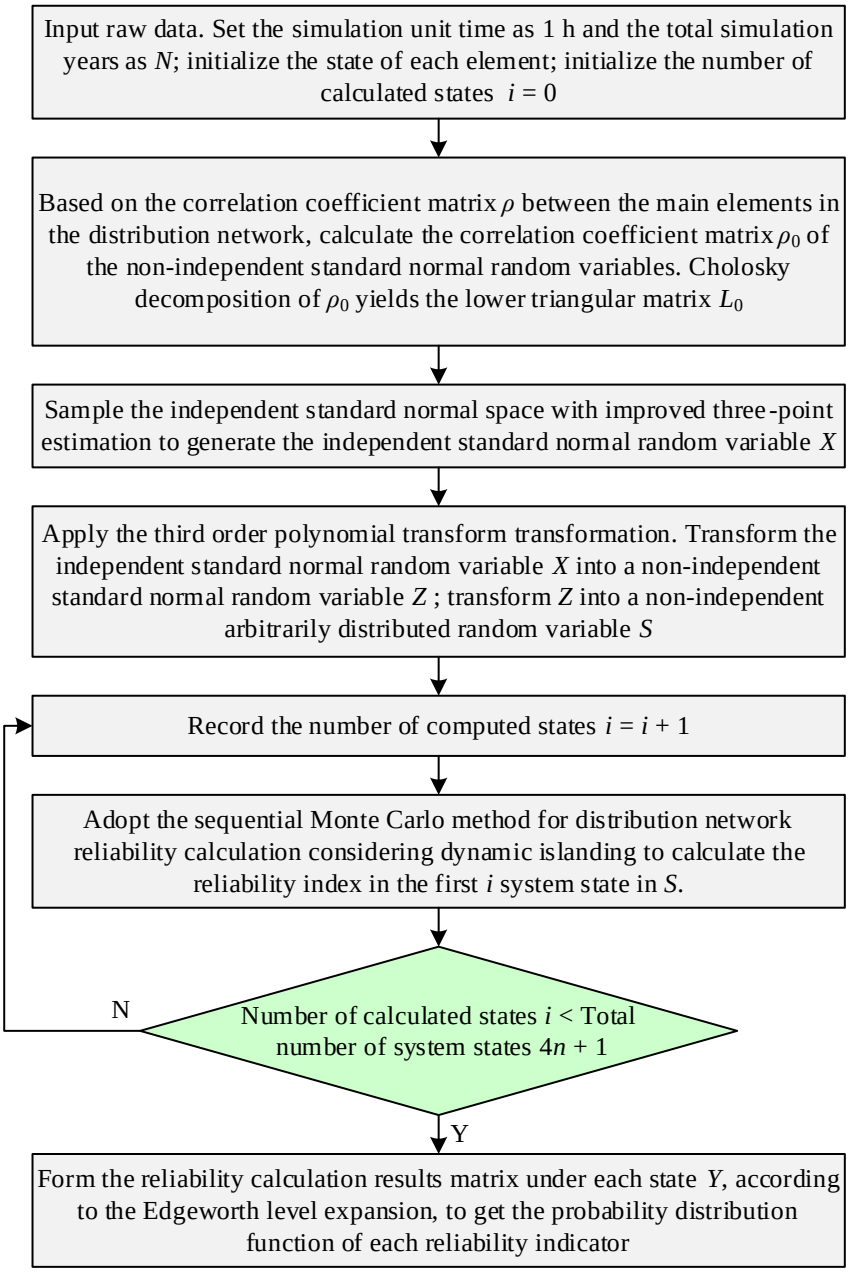

Figure 6: Distribution network probability reliability calculation process

4 Example calculation and analysis

4.1 Example System

The improved IEEE-RBTS Bus6 F4 feeder is taken as a test system in the current work to study the impact of distributed power access on voltage level and loss. After the addition of distributed

power to the system, the proposed methodology and the traditional Monte Carlo simulation method may be used to determine the probabilistic reliability of the distribution network. The state of operation of the distribution network in the conventional Monte Carlo analysis method will be evaluated and computed at each discrete time interval. That is how reliability indices of all states will be determined. Histogram of the calculation result is the probabilistic reliability, whereas the mean of the results is the expected reliability of the system.

The load data of the time series load model of the distribution system under study are based on the IEEE-RBTS-79 system. The time series load model is a combination of the system peak load which is used to compute the annual load profile. One sample of the annual load profile of the load point LP6 is illustrated in Figure 7. All load points have a correlation coefficient of 0.65.

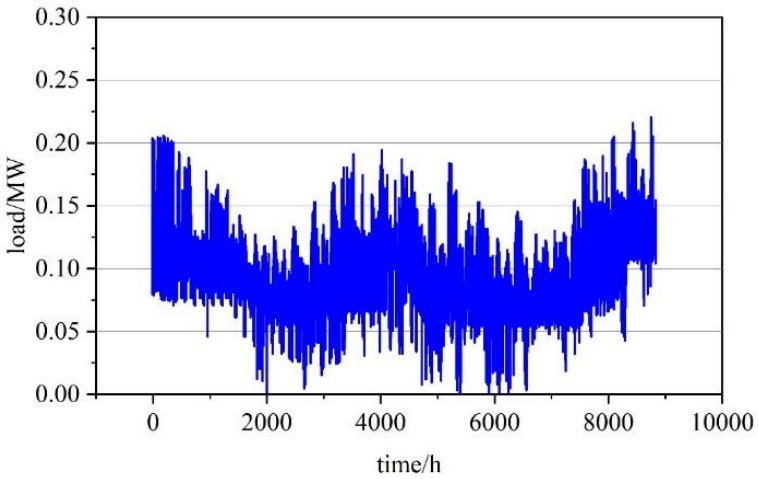

Figure 7: Load point lp6 in a year's timing changes

4.2 Sensitivity Calculations and Analysis

The purpose of sensitivity analysis in the sphere of power systems is to learn the tendencies of change and interaction between different factors that influence the voltage and losses of a network. Also, sensitivity analysis will offer some information about the limitations on the different variables impacting the voltage and losses. The presented sensitivity analysis will demonstrate how variables are influencing the voltage sensitivity and the network losses. Considering the point of view on the control of the voltage and network loss, the control theory may be applied to divide all the variables into three categories. The categories are control variables, state variables, and output variables. The active and reactive power of the power sources and active and reactive load powers, as control variables, impact the voltage and losses in the grid. Depending on the changing conditions of operation, the control variables might slightly or drastically change, and this would lead to changes in the state and output variables. Sensitivity analysis can be used to determine the voltage and network loss sensitivities with varying active and reactive powers in the sources and loads.

Taking into account the DG output for active power generation of 30 MW, 50 MW, and 70 MW, the influence of connecting a DG at node 12 to the system's node voltage and node-voltage deviation can be illustrated by Figures 8 and 9. Once the DG is connected, there is a noticeable rise in the node voltage level. As the active power generation of the DG increases, there is a noticeable rise in the voltage of the connected node. In other words, for a DG active power generation of 70 MW, the node voltage level is higher than that for a DG active power generation of 30 MW by 0.035 MW.

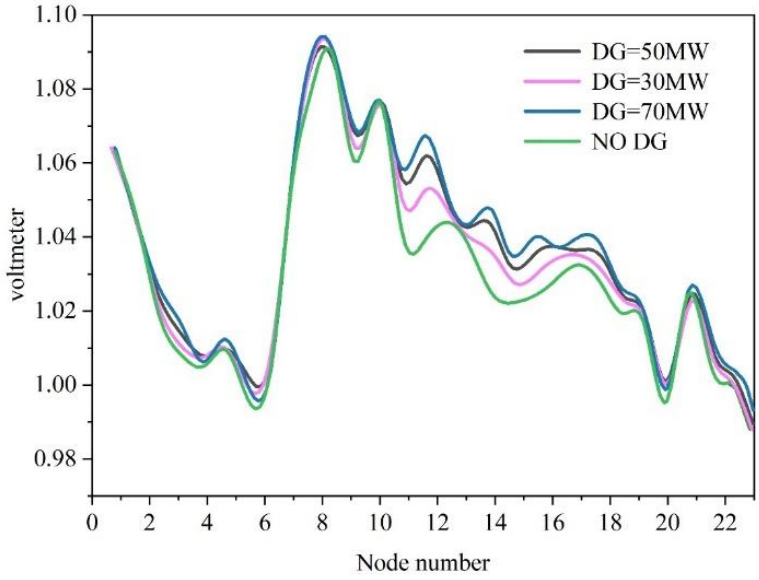

Figure 8: The effect of distributed power power on the node voltage

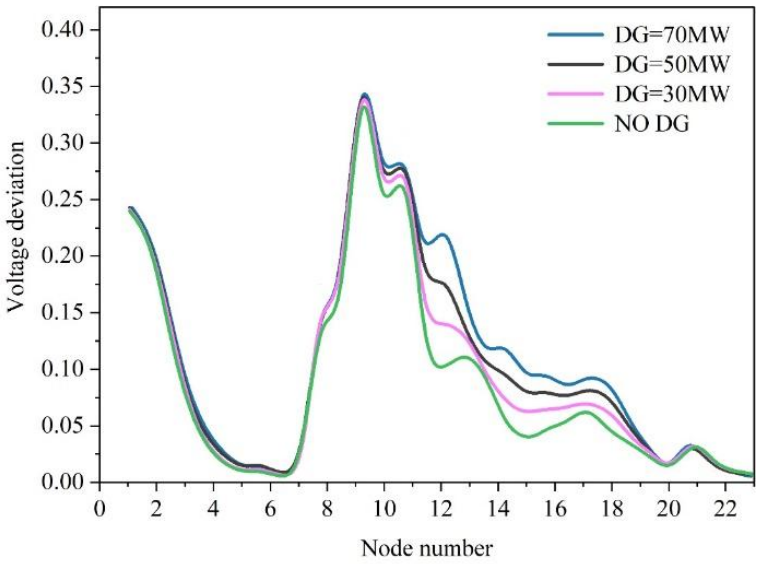

Figure 9: The effect of distributed power power on the voltage offset of nodes

Figure 10 depicts the effect of integrating DG into the power grid on active power losses on the line. As the amount of generated power increases, the loss of active power decreases in some lines (such as lines 1, 2, and 5), while it increases in other lines (for instance, lines 15 and 25). In sum, integrating distributed generation sources may lead to an increase or decrease in power losses in a power system. The ultimate effect depends on various criteria such as the connection point of the distributed generator, the proportion of the DG source compared to the power demand, and the network configuration.

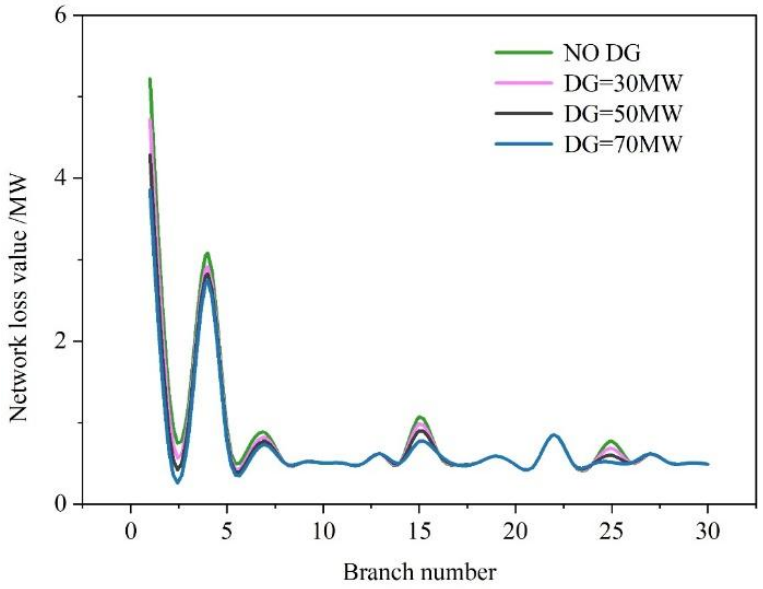

Figure 10: The effect of distributed power supply on net loss

4.3 Comparison of the results obtained using the method described in this paper with those obtained using traditional Monte Carlo methods

The calculation of load-point reliability measures and system reliability measures under the first correlation coefficient is done utilizing the approach suggested in this paper, as well as the standard Monte Carlo simulation approach. The time taken for each approach to execute is noted down, followed by the comparison of the outputs obtained from the new approach and the Monte Carlo approach.

4.3.1 Comparison of calculations for system reliability indicators

The system reliability metrics selected in this paper include SAIFI, SAIDI, CAIDI, ENS, and SASI. Among these, SAIFI, SAIDI, and CAIDI are interconvertible, so in the subsequent results presentation, only the mutually independent SAIFI and SAIDI are selected for display and analysis.

Table 1 shows the reliability metric calculation results and relative deviations obtained using the method proposed in this paper and the Monte Carlo method. The results obtained using the method proposed in this paper exhibit smaller relative deviations compared to those from the Monte Carlo method. The relative deviation for the ASAI metric reached 0.000%, and the largest deviation among all metrics was only 2.199%, indicating that the method proposed in this paper possesses high computational accuracy.

Table 1: The calculation results are compared and relative

Reliability indicator/unit	Monte carlo method	This method	The deviation of the method and the monte carlo method
SAIFI/(secondary /(user*Year))	1.05452	1.03651	1.708%
SAIDI/(h /(user*Year))	4.82541	4.73564	1.860%
ASAI/%	99.56412	99.56425	0.000%
ENS(kilowatt hour/year)	39.17412	38.31254	2.199%

The system reliability metrics selected in this paper include SAIFI, SAIDI, CAIDI, ENS,

and SASI. Among these, SAIFI, SAIDI, and CAIDI are interconvertible, so in the subsequent results presentation, only the mutually independent SAIFI and SAIDI are selected for display and analysis.

Table 1 presents reliability indices obtained by using the proposed technique along with their corresponding relative deviations when compared to the Monte Carlo technique. The deviations from the Monte Carlo simulation technique are lower with the proposed approach. More specifically, the relative deviation from the ASAI index is 0.000%, and the highest relative deviation from any other index is 2.199%.

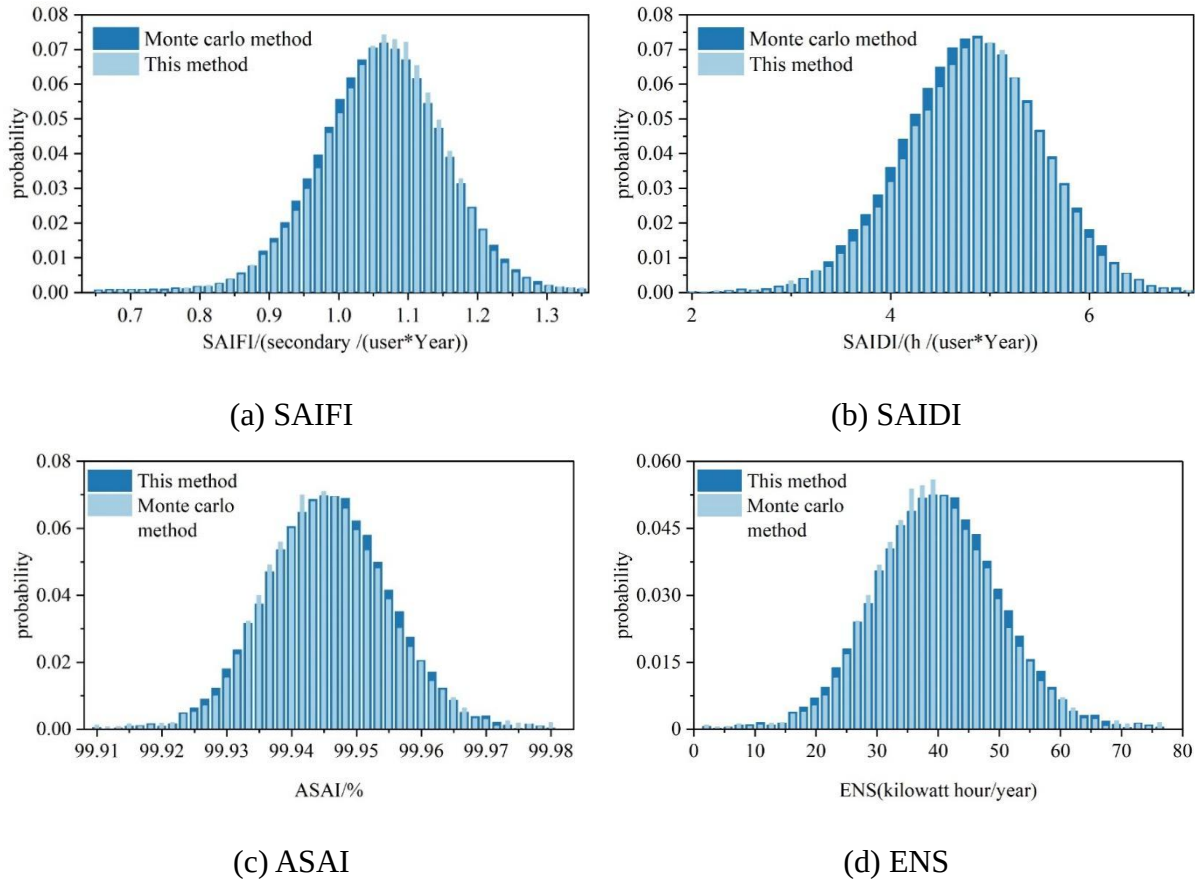

(a) SAIFI (b) SAIDI

(c) ASAI (d) ENS

Figure 11: The probability distribution of system reliability index is compared

4.3.2 Comparison of calculation results for load point reliability indicators

In the current research, a block including load points 2-8 is considered in order to determine the difference between the obtained mean values of load point indicators through the use of the proposed approach and the Monte Carlo approach. Figure 12 shows the comparison of indicator values for each load point in this block. Here figures (a)-(d) depict the values of λ, r, U, and ENS, respectively.

Differences between the reliability indicators of load points 2-8 found in this study with the use of the proposed approach and the Monte Carlo approach include the following: for λ = 1.561%, for r = 2.564%, for U = 2.112%, and for ENS = 0.854%. From these data, it becomes clear that minor differences arise in the calculation of the reliability indicators of load points using the proposed approach compared to the Monte Carlo approach.

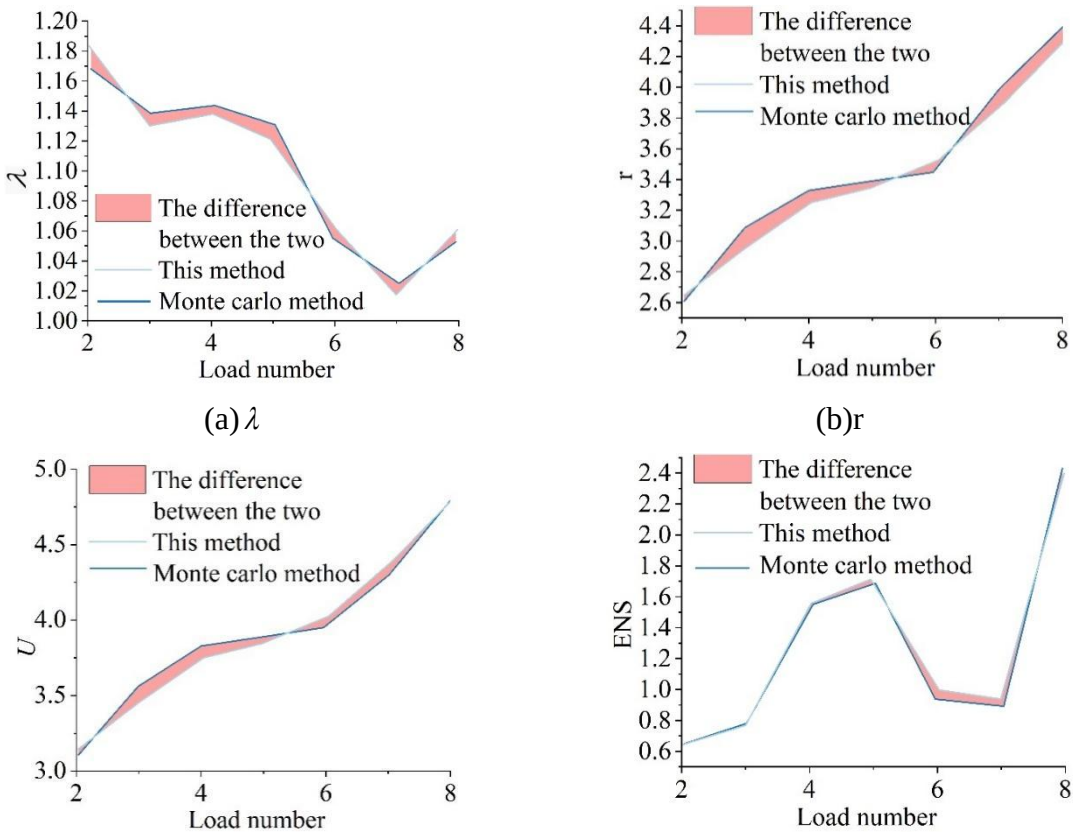

(a) λ (b)r

(c)U (d)ENS

Figure 12: The index of the load point is compared

5 Conclusion

In this study, a sensitivity analysis methodology through loop analysis in relation to distribution grids is provided. Moreover, this study offers an approach to assessing the probability of reliability through Monte Carlo. It is used to assess the change in reliability and sensitivity at each node after integrating distributed power sources into the distribution network.

(1) As the DG generation increases, different measures will react according to the system structure. For instance, with higher DG generation, the increase in voltage level becomes greater at the individual node. There exist differences in active power loss at the branch level. Branches 1, 2, and 5 witness reduced losses, whereas losses increase for branches 15 and 25. High penetration of distributed power sources can thus lead to decreased or increased system network losses after connecting to the distribution network. This method of calculating sensitivity offers an assessment of sensitivity change in protection device accurately and provides the theoretical basis and data support for protection device tuning.

(2) In contrast to the ordinary Monte Carlo method, Monte Carlo based probability-based reliability assessment for directional protection devices in high DG penetration of distribution network provides much smaller deviations. Relative deviation of ASAI is 0.000%, and maximum deviation among indexes is 2.199%. The reliability assessment approach provided in this paper achieves high accuracy when assessing the reliability of protection devices in distribution networks.

About the Author

Mou Xuepeng, (1982-), male, mxp_gzdw@163.com 18275184868, senior engineer, from Guizhou Power Grid Co., LTD. Research Center for Grid Planning, Master degree. His main research direction is power system operation and control.

Wang Jian, (1979-), male, 10031752@qq.com, 13885104515, senior engineer, from Guizhou Power Grid Co., LTD. Research Center for Grid Planning, Master degree. His main research direction is grid engineering consulting and evaluation.

Li Qingsheng, (1971-) male, lqs98@126.com, 13885185953, professor-level senior engineer, from Guizhou Power Grid Co., LTD. Grid Planning and Research Center, bachelor's degree, Main research direction: demand response, new energy storage, etc.

Funding

This work was supported by China Southern Power Grid Science and Technology Projects Construction of a Medium- and Low-Voltage Multi-Energy Panoramic Full-Scale Experimental Platform for New Distribution Systems (GZKJXM20220031)

References

[1] Dulău, L. I., Abrudean, M., & Bică, D. (2014). Distributed generation technologies and optimization. Procedia Technology, 12, 687-692.

[2] Filippov, S. P., Dilman, M. D., & Ilyushin, P. V. (2019). Distributed generation of electricity and sustainable regional growth. Thermal Engineering, 66(12), 869-880.

[3] Razavi, S. E., Rahimi, E., Javadi, M. S., Nezhad, A. E., Lotfi, M., Shafie-khah, M., & Catalão, J. P. (2019). Impact of distributed generation on protection and voltage regulation of distribution systems: A review. Renewable and Sustainable Energy Reviews, 105, 157-167.

[4] Jain, P., Poon, J., Singh, J. P., Spanos, C., Sanders, S. R., & Panda, S. K. (2019). A digital twin approach for fault diagnosis in distributed photovoltaic systems. IEEE Transactions on Power Electronics, 35(1), 940-956.

[5] Adefarati, T., Papy, N. B., Thopil, M., & Tazvinga, H. (2017). Non-renewable distributed generation technologies: A review. Handbook of Distributed Generation: Electric Power Technologies, Economics and Environmental Impacts, 69-105.

[6] Angelim, J. H., & Affonso, C. M. (2016). Impact of distributed generation technology and location on power system voltage stability. IEEE Latin America Transactions, 14(4), 1758-1765.

[7] Huang, Y., Jiang, Y., & Wang, J. (2021). Adaptability evaluation of distributed power sources connected to distribution network. IEEE Access, 9, 42409-42423.

[8] Kulmala, A., Repo, S., & Järventausta, P. (2014). Coordinated voltage control in distribution networks including several distributed energy resources. IEEE Transactions on Smart Grid, 5(4), 2010-2020.

[9] Ehsan, A., & Yang, Q. (2018). Optimal integration and planning of renewable distributed generation in the power distribution networks: A review of analytical techniques. Applied energy, 210, 44-59.

[10] Dorostkar-Ghamsari, M. R., Fotuhi-Firuzabad, M., Lehtonen, M., & Safdarian, A. (2015). Value of distribution network reconfiguration in presence of renewable energy resources. IEEE Transactions on Power Systems, 31(3), 1879-1888.

[11] Téllez, A. Á., López, G., Isaac, I., & González, J. W. (2018). Optimal reactive power compensation in electrical distribution systems with distributed resources. Review. Heliyon, 4(8).

[12] Martínez-Velasco, J. A., & Guerra, G. (2015). Analysis of large distribution networks with distributed energy resources. Ingeniare. Revista chilena de ingeniería, 23(4), 594-608.

[13] Galvez, C., & Abur, A. (2020). Fault location in active distribution networks containing distributed energy resources (DERs). IEEE Transactions on Power Delivery, 36(5), 3128-3139.

[14] Jiang, Y., Xu, J., Sun, Y., Wei, C., Wang, J., Liao, S., ... & Peng, X. (2018). Coordinated operation of gas-electricity integrated distribution system with multi-CCHP and distributed renewable energy sources. Applied energy, 211, 237-248.

[15] Bulychev, A. V., Okhotkin, G. P., Silanov, D. N., Vasiliev, S. A., & Alekseev, V. V. (2020). A Digital Relay Protection System in Electrical Distribution Networks. Russian Electrical Engineering, 91(8), 495-499.

[16] Prakash, K., Islam, F. R., Mamun, K. A., Lallu, A., & Cirrincione, M. (2017, December). Reliability of power distribution networks with renewable energy sources. In 2017 4th Asia-Pacific World Congress on Computer Science and Engineering (APWC on CSE) (pp. 187-192). IEEE.

[17] Zhang, K., Shi, W., Zhu, H., Dall'Anese, E., & Başar, T. (2018). Dynamic power distribution system management with a locally connected communication network. IEEE Journal of Selected Topics in Signal Processing, 12(4), 673-687.

[18] Johansson, P., Vendel, M., & Nuur, C. (2020). Integrating distributed energy resources in electricity distribution systems: An explorative study of challenges facing DSOs in Sweden. Utilities Policy, 67, 101117.

[19] Guzmán-Henao, J. A., Bolaños, R. I., Montoya, O. D., Grisales-Noreña, L. F., & Chamorro, H. R. (2024). On integrating and operating distributed energy resources in distribution networks: a review of current solution methods, challenges, and opportunities. IEEE Access, 12, 55111-55133.

[20] Quadri, I. A., Bhowmick, S., & Joshi, D. (2018). A comprehensive technique for optimal allocation of distributed energy resources in radial distribution systems. Applied energy, 211, 1245-1260.

[21] Li, Z., Shahidehpour, M., Alabdulwahab, A., & Al-Turki, Y. (2019). Valuation of

distributed energy resources in active distribution networks. The Electricity Journal, 32(4), 27-36.

[22] Jeddi, B., Vahidinasab, V., Ramezanpour, P., Aghaei, J., Shafie-khah, M., & Catalão, J. P. (2019). Robust optimization framework for dynamic distributed energy resources planning in distribution networks. International Journal of Electrical Power & Energy Systems, 110, 419-433.

[23] Agarwal, U., & Jain, N. (2019). Distributed energy resources and supportive methodologies for their optimal planning under modern distribution network: a review. Technology and Economics of Smart Grids and Sustainable Energy, 4(1), 3.

[24] Nsaif, Y. M., Lipu, M. H., Ayob, A., Yusof, Y., & Hussain, A. (2021). Fault detection and protection schemes for distributed generation integrated to distribution network: Challenges and suggestions. IEEE access, 9, 142693-142717.

[25] Dalin Mu,Guo Lei,Tingwei Xu,Haiqiang Zhang,Xiaopeng Li & Sheng Lin. (2025). Fault location scheme of HVDC converter based on fault loop analysis. International Journal of Electrical Power and Energy Systems, 168, 110701-110701.

[26] Han Hou, Hongchang Ding, Keyan Dong, Guohua Cao & Boyuan Wang. (2025). A Method for Mounting Space Telescope Optical Systems Based on the Sensitivity Matrix of Intrinsic Coefficients. Sensors, 25(4), 1121-1121.

[27] Ruihan Kan, Yanchun Xu, Zhenhua Li & Mi Lu. (2024). Calculation of probabilistic harmonic power flow based on improved three-point estimation method and maximum entropy as distributed generators access to distribution network. Electric Power Systems Research, 230, 110197-.

[28] Hao Lu & Zhencai Zhu. (2018). Reliability-based robust design optimization using anchored ANOVA expansion and truncated Edgeworth series approximation. Proceedings of the Institution of Mechanical Engineers, Part E: Journal of Process Mechanical Engineering, 232(4),408-417.